Modular Coil Design for the Ultra-Low Aspect Ratio Quasi-Axially Symmetric Stellarator MHH2

L. P. Ku and the ARIES-CS Team

Princeton Plasma Physics Laboratory, P. O. Box 451, Princeton, NJ 08543-0451

Abstract—**A family of two field-period quasi-axisymmetric stellarators generally known as MHH2 with aspect ratios of only ~2.5 was found. These configurations have low field ripples and excellent confinement of α particles. This discovery raises the hope that a compact stellarator reactor may eventually be designed with the property of tokamak transport and stellarator stability. In this paper we demonstrate that smooth modular coils may be designed for this family of configurations that not only yield plasmas with good physics properties but also possess engineering properties desirable for compact power producing reactors. We show designs featuring 16 modular coils with ratios of major radius to minimum coil-plasma separation ~5.5, major radius to minimum coil-coil separation ~10 and the maximum field in coil bodies to the field on axis ~2 for 0.2 m^2 conductors. These coils is expected to allow plasmas operated at 5% β with α energy loss < 10% for a reactor of major radius <9 m at 5 T.**

Keywords-stellarator; quasi-axisymmetry; fusion reactor; low aspect ratio; coil design

I. INTRODUCTION

During the course of ARIES-CS studies, we discovered a family of 2 field-period stellarator configurations, generally known as MHH2, in which the magnetic field structures may be optimized to be nearly toroidally symmetric and the plasma aspect ratio was only ~2.5 [1, 2]. They have low field ripples and good confinement of α particles. This raises the prospect of them being considered as the candidate for compact power producing reactors capable of operating in a steady-state at high beta with low re-circulating power and minimal disruptions.

The attractiveness of this "ultra-low" aspect ratio MHH2 as compact, small sized reactors can be realized only if coils can also be designed with sufficient compactness and with good engineering properties, however. For a reactor, sufficient space between the plasma and coils must be provided to accommodate the blanket for tritium breeding if deuterium and tritium (DT) are used as fusion fuels. Radiation shielding must also be in place for protection of coils. If the ratio of the major radius to the minimum coil to plasma separation gets small to leave more room for the first wall, blanket and shielding, the shape of the coils may become too complex to be attractive due to the fast decay of high order moments that are needed to shape the plasma. If the ratio gets large, the size of the machine may have to be increased to provide enough space and therefore the machine may become too big to be compact, irrespective of the compactness of the plasma itself. Typically, the minimum space required for DT fuel self-sufficiency and the protection of irreplaceable components of a reactor against

radiation damage during a 40 full-power-year operation is ~1.4 m (including plasma scrape-off, vacuum vessel, coil structure, manifold, etc.). In addition, the maximum magnetic field in the plasma, hence the power density, is limited by the maximum allowable field in the coil body, which in turn depends on the complexity of the coils and the type of conductor ultimately chosen. Coils must have adequate separation among themselves and sufficient radius of curvature throughout the winding. These considerations will allow for the ease of port installation, machine assembly and remote maintenance. The design optimization is made more challenging for MHH2 because the low aspect ratio makes the real estate inside the donut hole more precious.

In section II, we discuss the approaches and optimization techniques for designing modular coils for MHH2. In section III, we show one design example with 16 modular coils, illustrating the engineering properties and the physics properties as well, for plasmas that this coil set will be able to produce at 5% beta. In section IV, we give a summary and conclusions.

II. COIL DESIGN OPTIMIZATION

Coils that reproduce the desired plasma properties initially optimized by prescribing the plasma outmost boundary shape may be designed by requiring that normal components of the magnetic field on the last closed magnetic surface (LCMS) due to the coils cancel that due to the plasma current. Because of the discrete nature of coils, the normal field on the LCMS may not vanish exactly, but the errors may be minimized. Various techniques have been devised for this purpose [3, 4]. We use a three-stage approach: first, we solve for current potentials on a prescribed current carrying surface, from which an initial set of coils is cut; second, we allow the winding surface geometry as well as the geometry of the coils wound on this surface to vary so as not only to minimize the field errors on the LCMS but also to enforce additional constraints, such as minimum separations to the plasma or to the neighboring coils, to optimize the engineering properties; and finally, we directly solve for the free boundary equilibrium and optimize both the physics properties (QA, α loss, etc.) and engineering properties aforementioned simultaneously instead of minimizing the normal field error on the boundary defined by the original fixed boundary plasma to allow the extra degrees of freedom to locate a "better" optimum using coil parameters obtained from step 2 as the initial condition. The last step is a complicated and difficult procedure, but it is necessary because of the complexity of the coil geometry required to include all the

essential harmonics of the magnetic field to yield needed plasma properties.

Typically, we represent coils parametrically as two dimensional Fourier series in terms of toroidal and poloidal angles on a winding surface. The winding surface itself in turn is represented as Fourier series in the toroidal and poloidal angles. This double representation has the advantage in that it allows one to choose the initial coil geometry in a more flexible and intuitive way. It also allows a more efficient optimization than by specifying directly the Cartesian coordinates of the coils. The initial choice of the winding surface is important since the optimization is highly non-linear and the configuration space is complex with many valleys and hills. The optimization is to find the "local" minimum of the penalty function we specified. There is no unique solution in this multi-dimensional optimization. An optimal solution is such that all constraints are satisfied and the penalty function is minimized.

The initial choice of the winding surface is to make it resemble the last closed magnetic surface of the fixed-boundary plasma optimized with respect to the physics properties with an offset large enough to meet the separation constraint between the winding surface and coils and to set the outboard far enough to minimize the ripple caused by the discrete coils. To minimize the perturbation due to the discrete coils, we find that the average minor radius of the outboard surface needs to be at least twice as large as the average plasma minor radius.

For a DT reactor the tritium breeding and coil protection from radiation damage typically require a blanket and shield to have certain minimum thickness. We included the coil aspect ratio R/Δ_{min}(C-P) as a constraint in the design optimization, where R is the plasma major radius and Δ_{min}(C-P) is the minimum separation between the coils and the LCMS. In 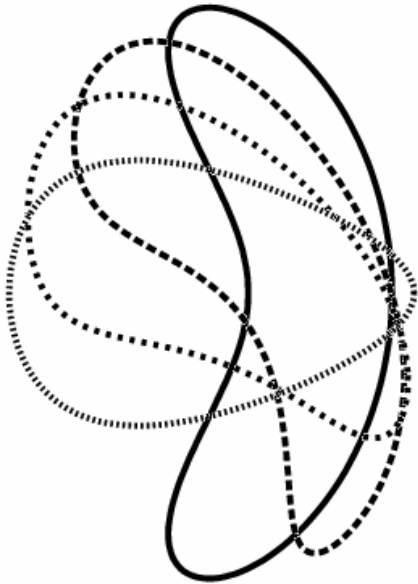addition, we impose the constraints of coil separation ratio R/Δ_{min}(C-C), where Δ_{min}(C-C) is the minimum separation among coils, and the minimum radius of curvature in the coil optimization. We allow coils to have different currents, but they have to maintain stellarator symmetry. Typically we search solutions for which the coil aspect ratio is <6, coil separation ratio < 12, and major radius to minimum radius of curvature <10. During the last stage of optimization in which free boundary equilibrium is solved, we vary the coil geometry as well as coil currents to minimize the non-axisymmetric "noise" in the magnetic spectrum, the effective ripples and the collisionless orbits of escaping α particles.

Typically, state variables consist of ~200 Fourier coefficients describing the coil geometry and location, and the penalty function consists of ~3000 physics and engineering constraints imposing acceptance criteria for QA and coil properties. The search of optimum in the design space is carried out by the Levenberg-Marquardt non-linear minimization technique [5]. VMEC [6] is used for the calculation of plasma equilibrium and NEO [7] and ORBIT3D [8] are used for the evaluation of effective helical ripples and the loss of α particles, respectively.

III.   A SIXTEEN MODULAR COIL DESIGN FOR MHH2

The configuration used as the basis of the coil design discussed here is called MHH2-K14 whose physics characteristics are detailed in [1]. Fig. 1 shows the last closed magnetic surface for which the coil design is intended to target. A typical design using only modular coils is illustrated in Fig. 2 which was obtained by the three steps of optimization with the increasing sophistication and complexity outlined in Section II. There are four distinct types of coils in each of the half periods with the coil aspect ratio 5.5 and coil separation ratio 10. The ratio of the plasma major radius to the minimum radius of curvature of these coils is about 13. It is seen in Fig. 2 that the coils are reasonably smooth, but in the inboard region near the crescent-shaped plasma at the beginning of a field period they are twisted to provide the push along the ridges.

One of the most important coil design parameters is the ratio of the maximum magnetic field in the coils to the field on the magnetic axis, B_{max}/B_0. The fusion power density is

Fig. 1.   The Last Closed Magnetic Surface (LCMS) shown in four equal toroidal sections in half a period for MHH-K14.
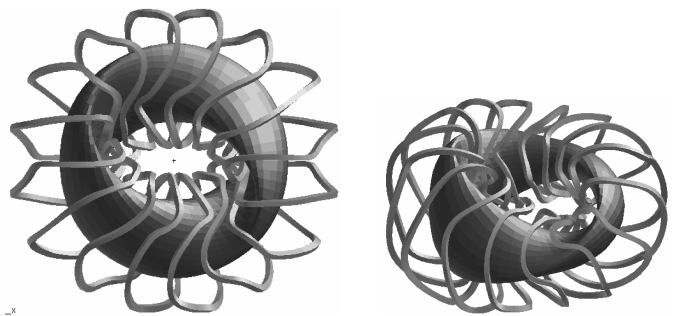

Fig. 2.   Top and perspective views of a modular coil design with coil aspect ratio 5.5. The LCMS of the plasma is also shown. There are four distinctive types of coils for a total of 16 coils in two field periods.
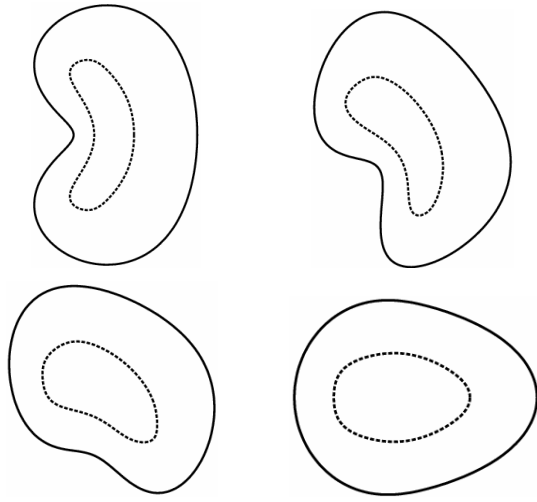
Fig. 3. Coil winding surface and the last closed magnetic surface of the free-boundary equilibrium at 5% β constructed from the coils using VMEC at four equally spaced toroidal plane over half-period.

proportional to B_0^4 for a given β, whereas the maximum achievable B_0 is limited by B_{max}/B_0 for a given type of conductor and current density. Our calculation indicates that $B_{max}/B_0 \sim 4.5$, 2.0, 1.5 for 0.2m x 0.2m, 0.4m x 0.4m and 0.6m x 0.6m conductors, respectively, for a reactor of size ~8 m in major radius with the coil design given in Fig. 2. The maximum coil current, when normalized to the field on axis and the major radius, is 0.316 MA/T-m. The variations of currents among the four types of coils are <5%. The area ratio of coil winding surface to the plasma surface is on the order of 2 and the coil lengths normalized to the plasma major radius typically range from 5.2 to 6.2.

To minimize the ripple from coil discretization, we initially prescribe the outer winding surface to be twice of the average minor radius. This enlarged space should also help providing rooms for remote handling and maintenance in a reactor. In Fig. 3 we show the optimized winding surface in relation to the LCMS of the equilibrium constructed from this set of coils at 5% β at four toroidal planes equally spaced over half a period enclosing the same amount of toroidal flux as that in Fig. 1. The flux surfaces indicate that the physics properties of the equilibrium are close to but not exactly the same as those for the fixed-boundary plasma shown in Fig. 1.

The fixed boundary equilibrium was optimized by prescribing a general rotational transform profile which is monotonically increasing. When optimizing coils by directly solving for free-boundary equilibrium, we first fit the current profile derived from the fixed-boundary calculation with the prescribed rotational transform and solve for free-boundary equilibria by constraining the current profile. Fig. 4 shows the rotational transform for both the external and internal component of the fixed- and free-boundary equilibria to illustrate the closeness of the two configurations. The plasma aspect ratios of the original fix-boundary equilibrium and the free-boundary equilibrium constructed using coils given in Fig. 2 with the same amount of enclosed toroidal flux are nearly

identical, 2.656 versus 2.659. The normalized plasma volume (volume/R^3 with R being the major radius) and surface area (area/R^2) are also very similar, 2.798 versus 2.793 for the volume and 18.895 versus 18.547 for the area. Moreover, with the free-boundary solution we are able to further optimize the quasi-axisymmetry. Fig. 5 shows the selected components in the magnetic spectrum of the equilibrium that the coil design is intended to reproduce and in the equilibrium that the coils actually produce. We see that the quasi-symmetry is improved, especially at r/a~0.7 where the non-axisymmetry goes through a minimum due to the mirror term crossing zero. The mirror term plays an important role in confining the energetic particle orbits, as we have observed in many occasions. Its presence, while not large, is significant. The overall effective ripple is not made worse due to its presence, however. The effective ripple is <0.8% in this configuration so that the neo-classical thermal transport should be negligible compared to the anomalous. The overall "noise", defined as the square root of the ratio of the magnetic energy due to the non-axisymmetric Fourier harmonics in the magnetic spectrum to that due to the axisymmetric components, is ~1% at r/a~0.7 for the fixed-boundary equilibrium, but it is only 0.4% for the free-boundary equilibrium. At the LCMS, they are 3.4% and 2.2%, respectively. The energy loss of α particle at 5% beta is expected to be ~5%, depending on the size and magnetic field
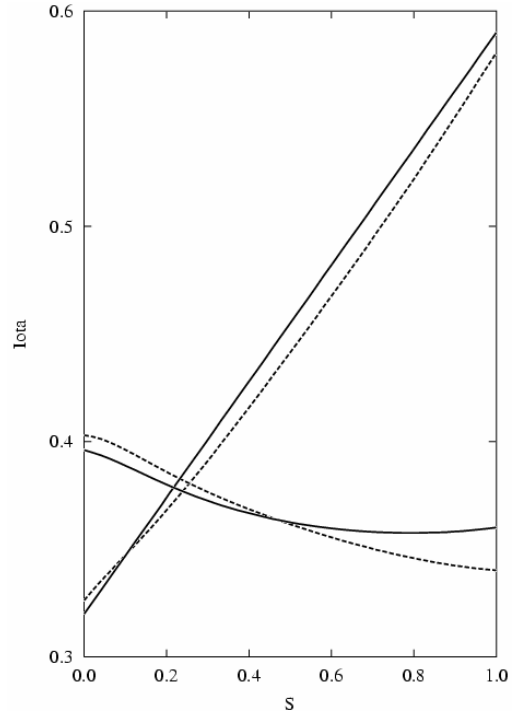

Fig. 4. External and total (including contribution from plasma current) rotational transforms plotted as function of the normalized toroidal flux S (~r^2/a^2). Solid lines are due to the original fixed-boundary equilibrium, dashed lines are due to the free-boundary equilibrium based on coils in Fig. 2. The external transforms are two curves with decreasing values as S increases and the total transform are two curves with monotonically increasing values as S increases. The equivalent magnitude of plasma current is 0.2 MA/T-m, corresponding to bootstrap current expected at 5% β.
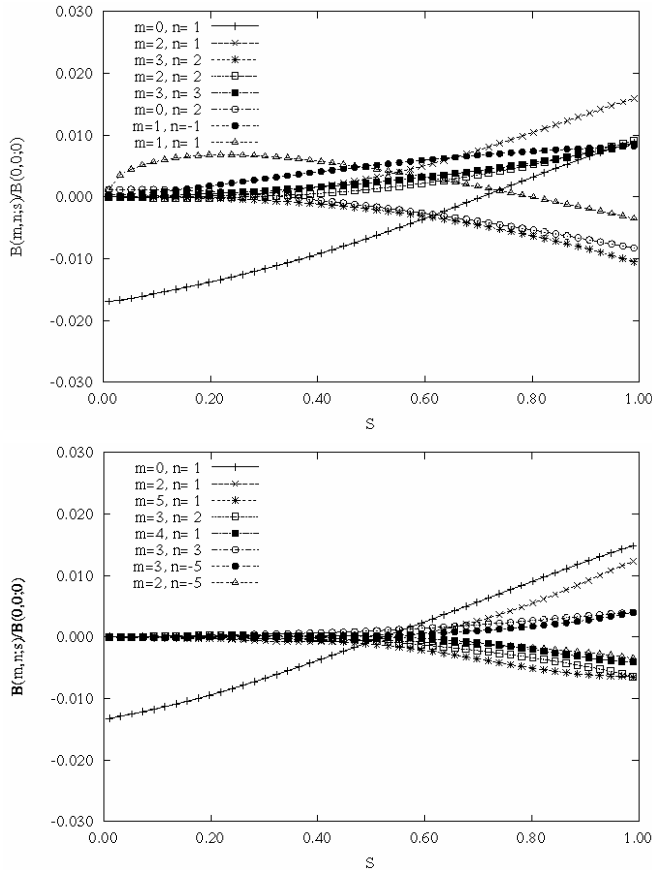
Fig. 5. Magnetic spectrum plotted as function of the normalized toroidal flux for the eight components having the largest magnitude. The top frame is for the fixed-boundary MHH2-K14 from which the present coils are derived. The bottom frame is for the free-boundary equilibrium obtained using the present coils. Note that except for the principal mirror term, the maximum non-axisymmetric component is only 1.2% and that the overall non-axisymmetry has a minimum at s~0.5, or r/a~0.7.
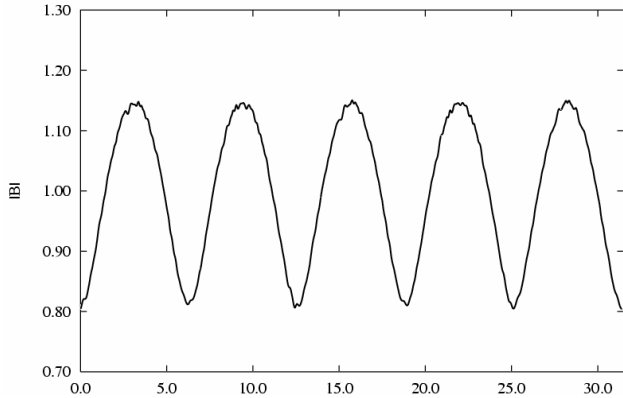

Fig. 6. Magnetic field strength plotted along a segment of field line on the surface at r/a=0.7 as function of θ starting from ϕ=0 and θ=0, where ϕ and θ are toroidal and poloidal angles, respectively, in Boozer coordinates.

residue is the lowest. The knot at r/a~0.7 in the magnetic spectrum appears to form a barrier for the loss of α particles.

IV. SUMMARY AND CONCLUSIONS

We have demonstrated that coils having properties desirable for a compact stellarator reactor exist for the low aspect ratio, quasi-axisymmetric configuration MHH2. These coils have sufficiently large distance from the plasma and have adequate separations among themselves. They are able to produce plasmas with sufficiently low field ripples and with good confinement of α particles. These results raise the hope that a compact device may be designed with tokamak transport and stellarator stability. Reactors of major radii < 9 m may be constructed that will produce 1 GWe of power when the plasma is at 5% β and 5 T.

REFERENCES

[1] L. P. Ku and the ARIES Team, "Reactor configuration development for ARIES-CS," 21th IEEE/NPSS Symposium on Fusion Engineering. Knoxville, Tennessee, September 26-29, 2005.

[2] P. R. Garabedian, L. P. Ku and the ARIES Team, "Reactors with stellarator stability and tokamak transport" Fusion Science and Technology, Vol. 47, No. 3, 400, April 2005.

[3] P. Merkel, "Solution of stellarator boundary value problems with external currents," Nucl. Fusion, Vol. 27, No. 5, 867, 1987.

[4] D. J. Strickler, L. A. Berry, and S. P. Hirshman, "Designing coils for compact stellarators," Fusion Science and Technology, Vol. 41, 107, March 2002.

[5] W. H. Press, S. A. Teukolsky, W. T Vetterling and B. P. Flannery, Numerical Recipes, The Art of Scientific Computing, 2nd Edition, Cambridge University Press, 1992.

[6] S. P. Hirshman , W. I. van Rij and P. Merkel, "Three-dimensional free boundary calculations using a spectral green's function method," Computer Physics Communications, 43, 143, 1986.

[7] V. V. Nemov, S. V. Kasilov, W. Kernbichler and M. F. Heyn, "Evaluation of 1/ν neoclassical transport in stellarators," Physics of Plasma, Vol. 6, No. 12, 4622, December 1999.

[8] R. B. White and M. S. Chance, "Hamiltonian guiding center drift orbit calculation for plasmas of arbitrary cross section," Phys. Fluids 27, 2455, 1984.

strength of the reactor. Indeed, examination of magnetic field strengths along field lines, an example of which is given in Fig. 6, indicates that there are only a small number of secondary ripple wells, particularly in regions near r/a~0.7, where the